MODELING DYNAMIC MAGNETICALLY INSULATED TRANSMISSION LINE FLOW IN A TRANSMISSION LINE CODE*

J.W. Schumer[ξ], P.F. Ottinger, D.D. Hinshelwood, and R.J. Allen
Pulsed Power Physics Branch, Plasma Physics Division, Naval Research Laboratory
Washington, DC 20375 USA

Abstract

A new fluid model including electron pressure is described for the electron flow layer in a magnetically insulated transmission line. Non-zero values of the electric field at the cathode are allowed so that the model can treat both emission and re-trapping of flow electrons. The model recovers previous results when the electric field at the cathode is taken to zero. The resulting generalized MITL flow equations are discussed and initial solutions are presented.

I. INTRODUCTION

Many modern pulsed power generators use magnetically insulated transmission lines (MITL) to couple power between the driver and the load [1]. In an MITL the electric field stress on the cathode exceeds the vacuum explosive-emission threshold and electron emission occurs. For sufficiently high current, emitted electrons are magnetically insulated from crossing the anode-cathode gap and flow axially downstream in the direction of power flow. The return current from the total anode current I_a is divided between current I_c flowing in the cathode and current I_f flowing in the vacuum electron layer, i.e., $I_f = I_a - I_c$. As a result of the electron flow in vacuum between the electrodes, the impedance of the MITL is altered and, thus, the power flow coupling between the machine and the load changes. The effective impedance is best described by the flow impedance Z_f [2,3]. In a dynamic system where the voltage and currents are changing in time, Z_f also varies [4].

The objective of the work is to efficiently and accurately simulate power flow in systems with a MITL using a simple TLC rather than a more computer intensive particle-in-cell code. A generalized model for flow impedance is developed for incorporation into a transmission line code (TLC), such as Bertha [5]. The model describes both self-limited flow as the pulse initially propagates down the MITL toward the load, as well as, the subsequent electron power flow along the MITL after the pulse encounters the load. Additionally, for low impedance loads (i.e., with impedance less than the self-limited impedance of the MITL), the flow is modified by the wave reflection off the load and the percentage of the return current in vacuum electron flow decreases. This phenomena is known as *electron re-trapping* [6] and must be included in a complete description of MITL flow.

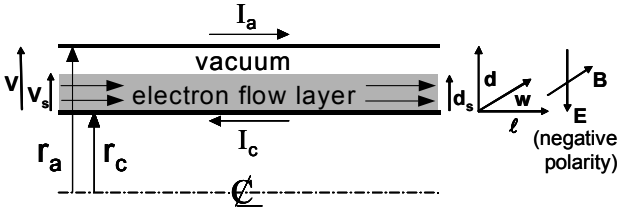

Figure 1. Schematic of MITL flow in planar geometry.

The approach is to develop a new fluid model for the electron layer which includes electron pressure. This modification extends MITL flow theory, allowing solutions with non-zero electric field at the cathode (i.e., $E_c \neq 0$) so that electron emission and re-trapping can be treated. A well-defined flow impedance is also derived. In addition, the pressure term is chosen appropriately to recover previous $E_c = 0$ solutions so that the results of the new rescaled MITL theory [3] can be applied. This newly extended MITL flow model may then be combined with time-dependent field equations [4] to build a dynamic model for MITL flow in a TLC. However, to complete the TLC model, a robust numerical technique must be constructed for solving these new MITL flow equations and techniques must be developed to treat special situations such as impedance transitions, adders, non-emitting regions (knobs), and load coupling,.

II. GENERALIZED MITL FLOW MODEL

In Fig. 1, negative-polarity MITL flow is illustrated where r_a and r_c would represent the anode and cathode radii in cylindrical geometry. For simplicity, the model is developed in planar geometry, considering a transmission line element of length ℓ, width w, and anode-cathode gap d. The three basic equations for the fluid model are the radial momentum transport equation, Poisson's equation, and Ampere's law, which are given by

* Work supported by the US Department of Energy through Sandia National Laboratories
ξ email: schumer@nrl.navy.mil

Report Documentation Page

Form Approved
OMB No. 0704-0188

1. REPORT DATE	2. REPORT TYPE	3. DATES COVERED
JUN 2007	**N/A**	**-**

4. TITLE AND SUBTITLE	5a. CONTRACT NUMBER
Modeling Dynamic Magnetically Insulated Transmission Line Flow In A Transmission Line Code	5b. GRANT NUMBER
	5c. PROGRAM ELEMENT NUMBER
6. AUTHOR(S)	5d. PROJECT NUMBER
	5e. TASK NUMBER
	5f. WORK UNIT NUMBER
7. PERFORMING ORGANIZATION NAME(S) AND ADDRESS(ES) **Pulsed Power Physics Branch, Plasma Physics Division, Naval Research Laboratory Washington, DC 20375 USA**	8. PERFORMING ORGANIZATION REPORT NUMBER
9. SPONSORING/MONITORING AGENCY NAME(S) AND ADDRESS(ES)	10. SPONSOR/MONITOR'S ACRONYM(S)
	11. SPONSOR/MONITOR'S REPORT NUMBER(S)

12. DISTRIBUTION/AVAILABILITY STATEMENT
Approved for public release, distribution unlimited

13. SUPPLEMENTARY NOTES
See also ADM002371. 2013 IEEE Pulsed Power Conference, Digest of Technical Papers 1976-2013, and Abstracts of the 2013 IEEE International Conference on Plasma Science. IEEE International Pulsed Power Conference (19th). Held in San Francisco, CA on 16-21 June 2013., The original document contains color images.

14. ABSTRACT
A new fluid model including electron pressure is described for the electron flow layer in a magnetically insulated transmission line. Non-zero values of the electric field at the cathode are allowed so that the model can treat both emission and re-trapping of flow electrons. The model recovers previous results when the electric field at the cathode is taken to zero. The resulting generalized MITL flow equations are discussed and initial solutions are presented.

15. SUBJECT TERMS

16. SECURITY CLASSIFICATION OF:			17. LIMITATION OF ABSTRACT	18. NUMBER OF PAGES	19a. NAME OF RESPONSIBLE PERSON
a. REPORT	b. ABSTRACT	c. THIS PAGE			
unclassified	**unclassified**	**unclassified**	**SAR**	**5**	

$$\frac{\partial T}{\partial x} = \rho(E - v_z B), \quad (1)$$

$$\frac{\partial E}{\partial x} = \frac{\rho}{\varepsilon_0}, \quad (2)$$

$$\frac{\partial B}{\partial x} = \mu_0 \rho v_z. \quad (3)$$

Here, T is the xx component of the electron pressure tensor, ρ is the electron charge density, v_z is the axial electron fluid velocity, E and B are the electric and magnetic fields, and ε_0 and μ_0 are the permittivity and permeability of free space, respectively. As expressed in Eqs. (1) – (3), ρ, v_z, T, and B are all positive-definite quantities, while E is positive at the anode but can be positive or negative at the cathode. Note that, because the time derivatives have been assumed negligible, this is a quasi-equilibrium model. The subscripts *c*, *s*, and *a* will denote quantities evaluated on the cathode at x = 0, electron layer edge at x = d_s, and anode at x = d, respectively. The vacuum impedance of the line is given by $Z_0 = c\mu_0 d/w$ where $c = 1/(\varepsilon_0\mu_0)^{1/2}$ is the speed of light. Also, anode and cathode fields are given by $E_{a,c} = Z_0 cQ_{a,c}/d$ and $B_{a,c} = Z_0 I_{a,c}/cd$, where $Q_{a,c}$ and $I_{a,c}$ are the charge per unit length and current (on the anode and cathode), respectively.

The voltage in the gap is given by

$$V(x) = \int_0^x E(x')dx' \quad , \quad (4)$$

where $V_c = V(0) = 0$ and the full voltage across the gap is V = V(d) (with the subscript *a* suppressed for simplicity). Similarly, the magnetic vector potential in the gap is given by

$$A(x) = \int_0^x B(x')dx' \quad , \quad (5)$$

where $A_c = A(0) = 0$ and the vector potential at the anode is A = A(d) (again with the subscript *a* suppressed). Both V and A will be needed for a complete description of the problem.

Because electron space-charge and current are distributed in the line, there is not, in general, a well-defined impedance. The electric flow impedance Z_f and the magnetic flow impedance Z_m are defined by the centroid of the space-charge and current, respectively [2]. By assuming here that both the charge density and axial fluid velocity are uniform in the flow layer, a well-defined flow impedance is derived with $Z_f = Z_m$. This assumption also makes integration of the above equations straightforward. However, without the $\partial T/\partial x$ pressure term, Eq. (1) cannot be satisfied under this assumption. Unlike the parapotential flow model [7] in which all electrons move axially in straight-line orbits, this model permits various orbit types [8]. The electron pressure is a consequence of the motion perpendicular to the axial flow which results from the distribution of electrons with these various orbits.

The MITL equations derived from this model are

$$I_a^2 - I_c^2 = c^2 Q_a^2 - c^2 Q_c^2, \quad (6)$$

$$V = Z_f cQ_a + (Z_0 - Z_f)cQ_c, \quad (7)$$

$$cA = Z_f I_a + (Z_0 - Z_f)I_c, \quad (8)$$

$$V = Z_0 cQ_a - \left(\frac{gmc^2}{2e}\right)\frac{(cQ_a - cQ_c)^2}{I_c^2}, \quad (9)$$

where m and e are the electron charge and mass, and g is a scaling parameter defined in [3]. In deriving these equations, the pressure at the cathode was chosen so that the previous MITL equations with $Q_c = 0$ are recovered [2-4].

Typically, Eq. (6) is referred to as the *pressure balance equation* and Eq. (9) is referred to as the *voltage equation*. When $Q_c = 0$ (i.e., $E_c = 0$), Eqs. (6) and (9) can be combined to yield the traditional *voltage equation*

$$V = Z_0 (I_a^2 - I_c^2)^{1/2} - \left(\frac{gmc^2}{2e}\right)\frac{(I_a^2 - I_c^2)}{I_c^2}, \quad (10)$$

which is used to calculate the voltage from measuring I_a and I_c. Previously, Eq. (10) was derived by postulating an expression for the charge density in the flow layer. Here, it is derived directly from the fluid model.

The model also yields

$$Z_f = Z_0\left(1 - \frac{d_s}{2d}\right), \quad (11)$$

so that $Z_0 \geq Z_f \geq Z_0/2$ for an electron layer thickness d_s ranging from 0 to d. Additionally, the charge density in the electron layer ρ, the axial fluid velocity in the electron layer v_z, the electron layer thickness d_s, the voltage at the edge of the electron layer V_s, and the magnetic vector potential at the edge of the electron layer A_s are given by

$$\rho = \frac{e\varepsilon_0 Z_0^2 I_c^2}{gmc^2 d^2}, \quad (12)$$

$$\frac{v_z}{c} = \frac{(I_a - I_c)}{(cQ_a - cQ_c)}, \quad (13)$$

$$\frac{d_s}{d} = \left(\frac{gmc^2}{eZ_0}\right)\frac{(cQ_a - cQ_c)}{I_c^2}, \quad (14)$$

$$\frac{eV_s}{gmc^2} = \frac{(c^2 Q_a^2 - c^2 Q_c^2)}{2I_c^2}, \quad (15)$$

and

$$cA_s = (Z_0 - Z_f)(I_a + I_c). \quad (16)$$

Finally, Eqs. (7) and (9) can be combined to provide

$$Z_f = Z_0 - \left(\frac{gmc^2}{2e}\right)\frac{(cQ_a - cQ_c)}{I_c^2}, \qquad (17)$$

which for $cQ_c = 0$ again yields the traditional result [3]

$$Z_f = Z_0 - \left(\frac{gmc^2}{2e}\right)\frac{(I_a^2 - I_c^2)^{1/2}}{I_c^2}. \qquad (18)$$

In practice, the dynamic MITL model will receive advanced values of V, I_a, and A along the line for each time step from the TLC, where A is advanced using Eq. (11a) from [4]. Then, Eqs. (6) - (9) are used to solve for cQ_a, cQ_c, I_c, and Z_f to determine the flow along the line for the subsequent time step. The continuity equation

$$J_a = -\frac{\partial Q_a}{\partial t} - \frac{\partial I_a}{\partial z} \qquad (19)$$

is used to calculate current lost to the anode, where J_a is the linear current density and $I_{loss} = c\tau J_a$ is the loss current for a TLC element of length τ (in seconds).

III. SOLUTIONS

The TLC model for MITL flow depends on a robust numerical technique for solving Eqs. (6) – (9). The equations can be normalized to the local vacuum impedance Z_0 of the particular TLC element under consideration. Thus, Z_0cQ_a, Z_0cQ_c, Z_0I_c, and Z_f/Z_0 are the unknowns and V, Z_0I_a, and cA are the known parameters. Equations (6) – (9) can be combined to give a quintic equation in Z_0cQ_a, which may have 1, 3 or 5 real roots. Valid roots are restricted to physically-meaningful regions of parameter space.

To map out this parameter space, one may focus on solutions in which $Z_0cQ_c = 0$ (from traditional equilibrium MITL theory). First, the traditional Z_0I_a versus Z_0I_c solutions for the $Z_0cQ_c = 0$ is displayed in Fig. 2 for V = 6 MV. Also shown is cA versus Z_0I_a, which is derived from Eq. (8) with $Z_0cQ_c = 0$. Although both Z_0I_c and cA are really functions of Z_0I_a, the axes have been oriented with the independent variable on the *vertical axis* in order to display the results in the traditional manner. There is a one to one correspondence between these two solutions with the example indicated by the arrow in Fig. 2 corresponding to the solution in Fig. 3 for cA = 7.5 MV. Over most of the range of cA, only one $Z_0cQ_c = 0$ solution exists. However, over a narrow range of cA, there is a region where two solutions with different Z_0I_a values exists, corresponding to the region left of the minimum on the Z_0I_a versus Z_0I_c curve. This is traditionally referred to as the saturated-flow region.

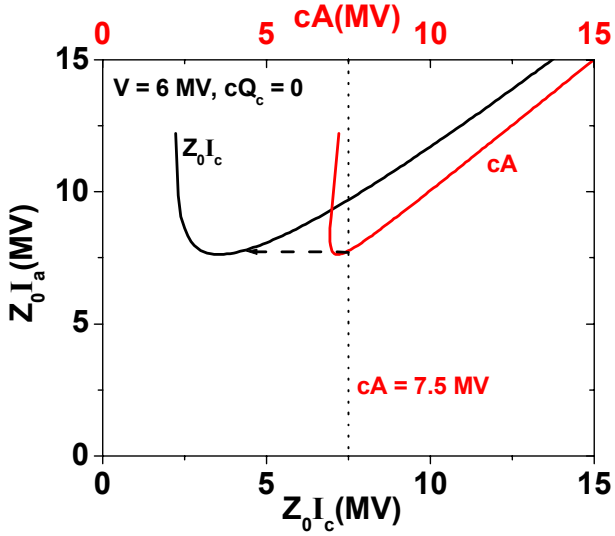

Figure 2. Plots of Z_0I_c and cA as functions of Z_0I_a for V = 6 MV with $Z_0cQ_c = 0$.

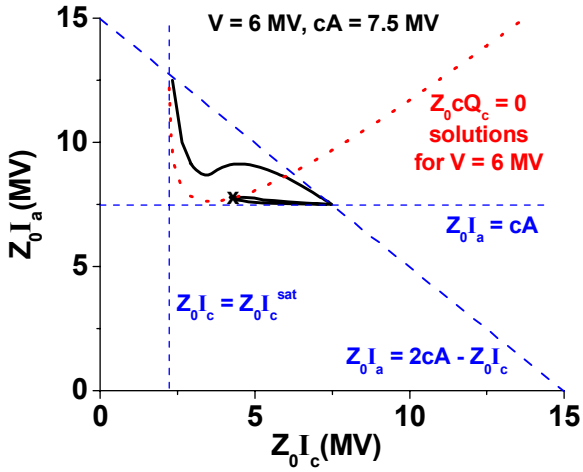

Figure 3. Plot of Z_0I_c solutions as a function of Z_0I_a for the case with V = 6 MV and cA = 7.5 MV.

As an example of general solutions (i.e., with Z_0cQ_c not necessarily equal to zero), consider solutions for V = 6

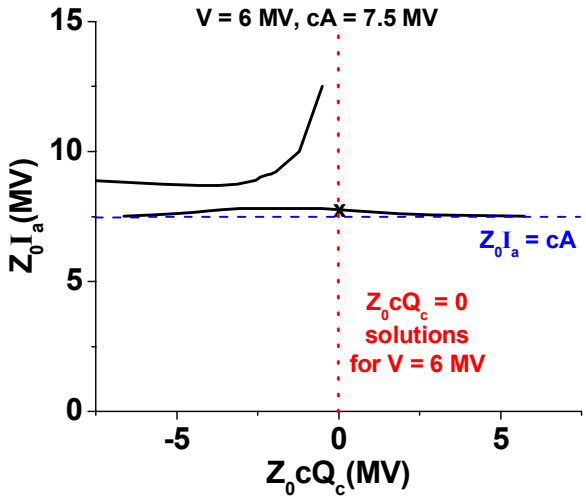

Figure 4. Plot of Z_0cQ_c solutions as a function of Z_0I_a for the case with V = 6 MV and cA = 7.5 MV.

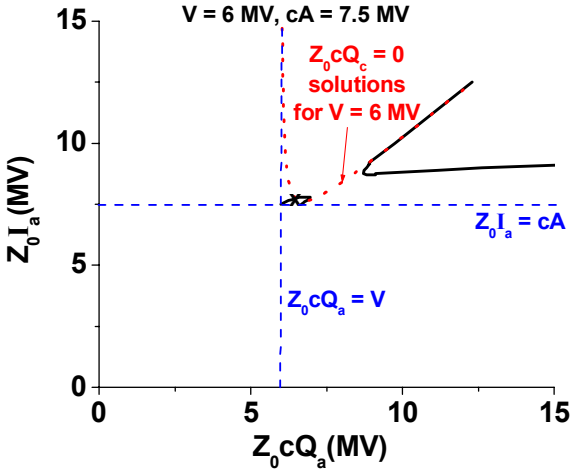

Figure 5. Plot of Z_0cQ_a solutions as a function of Z_0I_a for the case with V = 6 MV and cA = 7.5 MV.

MV and cA = 7.5 MV as a function of Z_0I_a. This value of cA occurs in Fig. 2 in a region where there is only oneZ_0I_a solution with $Z_0cQ_c = 0$. Solutions for Z_0I_c are shown in Fig. 3. Again, the axes are oriented to show the familiar Z_0I_a versus Z_0I_c curve. The straight dashed lines indicate bounding constraints on the solutions; thus, only solutions with values that fall within the triangular region are meaningful. These bounds are determined by $Z_0 \geq Z_f \geq Z_0/2$, $I_a \geq I_c$, and the constraints derived from these conditions.

Also note the traditional $Z_0cQ_c = 0$ solutions, indicated by the dotted curve in Fig. 3. Imagining that there is a Z_0cQ_c axis projecting in and out of the paper and that solutions with different values of Z_0cQ_c are projected onto the plane of the paper, the only solution with $Z_0cQ_c = 0$ occurs at the location indicated by the "x". Note that this solution falls on the dotted $Z_0cQ_c = 0$ curve and corresponds to the solution indicted by the arrow in Fig. 2 for cA = 7.5 MV. Other points that seem to cross the $Z_0cQ_c = 0$ curve actually lie off the plane of the paper with $Z_0cQ_c \neq 0$.

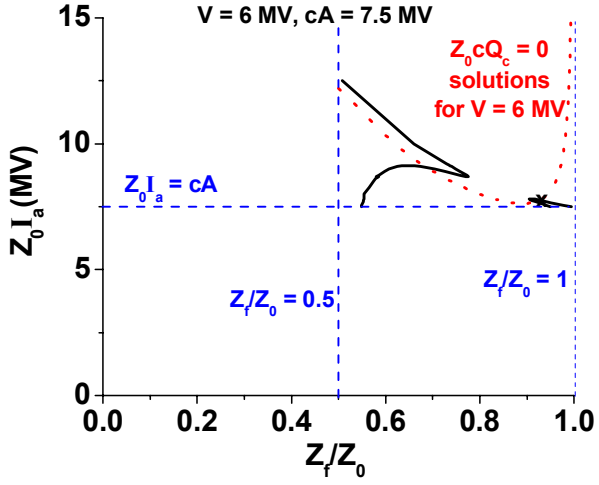

Figure 6. Plot of Z_f/Z_0 solutions as a function of Z_0I_a for the case with V = 6 MV and cA = 7.5 MV.

Solutions for Z_0cQ_c, Z_0cQ_a, and Z_f/Z_0 as functions of Z_0I_a are shown in Figs. 4, 5, and 6, respectively. For ease of comparison, the axes are also oriented in the same fashion as Fig. 2. In Fig. 4 the only $Z_0cQ_c = 0$ solution for these values of V and cA occurs on the lower branch. Note that when $Z_0cQ_c > 0$ (i.e., $E_c > 0$), electron emission occurs at the cathode, and when $Z_0cQ_c < 0$ (i.e., $E_c < 0$), electron re-trapping occurs. Also note that Z_0I_c and Z_0cQ_c change rapidly near the $Z_0cQ_c = 0$ solution for small changes in Z_0I_a, while Z_0cQ_a and Z_f/Z_0 do not. This suggests that strong emission or re-trapping will tend to keep solutions in the vicinity of the $Z_0cQ_c = 0$ solutions at least when the flow is on this lower branch.

IV. SUMMARY

A fluid model has been developed to model generalized MITL flow. By explicitly including pressure in the model, the voltage equation can be derived directly rather than resulting from postulating an expression for the density in the flow layer as was previously done. By allowing solutions with $E_c \neq 0$, emission and re-trapping can be treated. By assuming that both the charge density and axial fluid velocity are uniform in the flow layer, a well-defined flow impedance is derived with $Z_f = Z_{in}$. This assumption is allowable due to the inclusion of a pressure term in the fluid model. And, finally, by choosing the form of the pressure term appropriately, the model reproduces the new rescaled MITL flow model when E_c (or equivalently Q_c) is taken to zero. This newly extended MITL flow model may be combined with time-dependent field equations to build a dynamic model for MITL flow in a TLC. A robust numerical technique is being constructed to solve these new generalized MITL flow equations, however, techniques to treat impedance transitions, adders, non-emitting regions, load coupling, etc. are also needed to complete the TLC model.

V. REFERENCES

[1] J.P. VanDevender, J.T. Crow, B.G. Epstein, D.H. McDaniel, C.W. Mendel, E.L. Neau, J.W. Poukey, J.P. Quintenz, D.B. Seidel, and R.W. Stinnett, "Self-magnetically insulated electron flow in vacuum trans-mission lines," Physica, vol. 104C, pp. 167-182, 1981.
[2] C.W. Mendel and S.E. Rosenthal, "Modeling magnetically insulated devices using flow impedance," Phys. Plasmas, vol. 2, pp. 1332-1342, Apr. 1995.
[3] P.F. Ottinger and J.W. Schumer, "Rescaling of equilibrium magnetically insulated flow theory based on particle-in-cell simulations," Phys. Plasmas, vol. 13, p. 063109-1 – 063109-17, Jun. 2006.
[4] C.W. Mendel and S.E. Rosenthal, "Dynamic modeling of magnetically insulated transmission line systems," Phys. Plasmas, vol. 3, pp. 4207-4219, Nov. 1996.
[5] D.D. Hinshelwood, "Bertha – a versatile transmission

line and circuit code," NRL Memorandum Report 5185, Nov. 21, 1983.
[6] V.L. Bailey, P.A. Corcoran, D.L. Johnson, I.D. Smith, J.E. Maenchen, K.D. Hahn, I. Molina, D.C. Rovang, S. Portillo, E.A. Puetz, B.V. Oliver, D.V. Rose, D.R. Welch, D.W. Droemer, and T.L. Guy, "Re-trapping of vacuum electron current in magnetically insulated transmission lines," in Proc. of 15th Inter. Conf. on High-Power Particle Beams, St. Petersburg, Russia, Jul. 2004, pp. 247-250.
[7] J.M. Creedon, "Relativistic Brillouin flow in the high ν/γ diode," Appl. Phys., vol. 46, pp. 2946-2955, Jul. 1975.
[8] C.W. Mendel, D.B. Seidel, and S.A. Slutz, "A general theory of magnetically insulated electron flow," Phys. Fluids, vol. 26, pp. 3628-3535, Dec. 1983.